ACS OMEGA

Open Access

http://pubs.acs.org/journal/acsodf

Article

Synthesis, Characterization, and Antimicrobial Activity of Urea-Containing α/β Hybrid Peptides against *Pseudomonas aeruginosa* and Methicillin-Resistant *Staphylococcus aureus*

Shifa Firdous,[‖] Aminur Rahman Sarkar,[‖] Rakshit Manhas, Rubina Chowdhary, Arti Rathore, Jyoti Kumari, Rajkishor Rai,* and Avisek Mahapa*

Cite This: *ACS Omega* 2025, 10, 2102−2115

Read Online

ACCESS | Metrics & More | Article Recommendations | Supporting Information

ABSTRACT: The insertion of β-amino acids and replacement of the amide bond with a urea bond in antimicrobial peptide sequences are promising approaches to enhance the antibacterial activity and improve proteolytic stability. Herein, we describe the synthesis, characterization, and antibacterial activity of short $\alpha\beta$ cationic hybrid peptides LA^{U}-Orn-$\beta^{3,3}$Ac$_6$c-PEA, **DY-01**; LA^{U}-Lys-$\beta^{3,3}$Ac$_6$c-PEA, **DY-02**; and LA^{U}-Arg-$\beta^{3,3}$Ac$_6$c-PEA, **DY-03** in which a C12 lipid chain is conjugated at the N terminus of peptide through urea bonds. Further, we evaluated all the peptides against both *Pseudomonas aeruginosa* and methicillin-resistant *Staphylococcus aureus* (MRSA) and their multidrug resistant (MDR) clinical isolates. All of the peptides exhibited significant bactericidal efficacy with minimal inhibitory concentration (MIC) values ranging from 2.5 to 6.25 μM (1.4 to 3.9 μg/mL) against *P. aeruginosa* and its MDR clinical isolates, whereas the MIC values ranging from 0.78 to 6.25 μM (0.45 to 3.9 μg/mL) against MRSA and MDR clinical isolates of *S. aureus*. To understand the potency and mechanism of action of **DY-01** to **DY-03**, time-kill kinetics, biofilm inhibition and disruption, synergistic interactions with standard antibiotics, swarming motility, scanning electron microscopy (SEM) analyses, and ex vivo infection assay were performed. The SEM images revealed that all of the peptides exert antibacterial activity through a membrane disruption mechanism. Additionally, negligible cytotoxicity was observed against mammalian cell lines RAW 264.7 and J774A.1, with mild hemolysis at higher concentrations. The comprehensive antimicrobial assessments of **DY-01** to **DY-03** against *P. aeruginosa* and MRSA highlight their potential for clinical applications in combating resistant microbial infections.

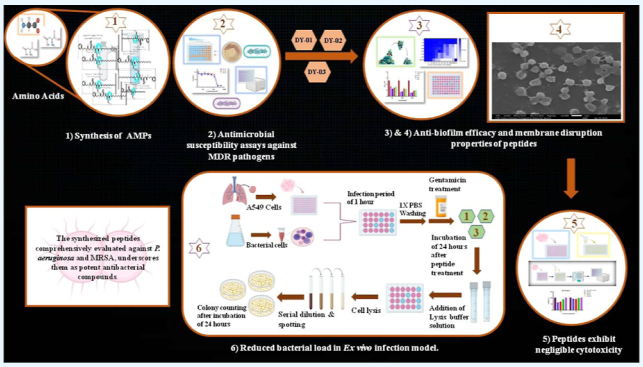

INTRODUCTION

Antimicrobial resistance (AMR) is a critical and multifaceted paradigm in microbial research that demands urgent attention. In recent decades, the emergence and spread of multidrug resistant (MDR) bacterial pathogen-associated infections have significantly increased, presenting a major challenge to public health. These MDR pathogens employ multiple mechanisms to circumvent the effects of drugs, leading to treatment failures and the spread of nosocomial infections.[1] The current necessity in the healthcare system is to formulate novel antimicrobials using advanced strategies and improved drug designs for effective results.

Antimicrobial peptides (AMPs) are small bioactive peptides that provide innate immunity in various multicellular organisms to combat pathogens.[2,3] AMPs offer a powerful alternative in antimicrobial drug discovery to combat AMR. They are gaining significant traction as a potent antimicrobial agent due to their potential antimicrobial activity, low tendency to confer resistance, and significant selectivity for targeting pathogens.[4] Unlike traditional antibiotics, AMPs often attack pathogens by disrupting and perforating bacterial membranes or interfering with intracellular processes, reducing the likelihood of resistance development.[2,3,5,6] Apart from membrane disruption, AMPs employ several other mechanisms, including inhibiting DNA replication, protein synthesis, cell wall synthesis, and cellular enzymes, as well as suppressing cellular transport through protein aggregation.[3] Additionally, AMPs play versatile roles beyond direct antimicrobial action, such as modulating immune responses, enhancing chemokine production, and supporting wound healing.[4] The development of synthetic peptides is considered a promising alternative to traditional antibiotics in combating MDR pathogens. These

Received: September 21, 2024
Revised: November 8, 2024
Accepted: November 22, 2024
Published: January 8, 2025

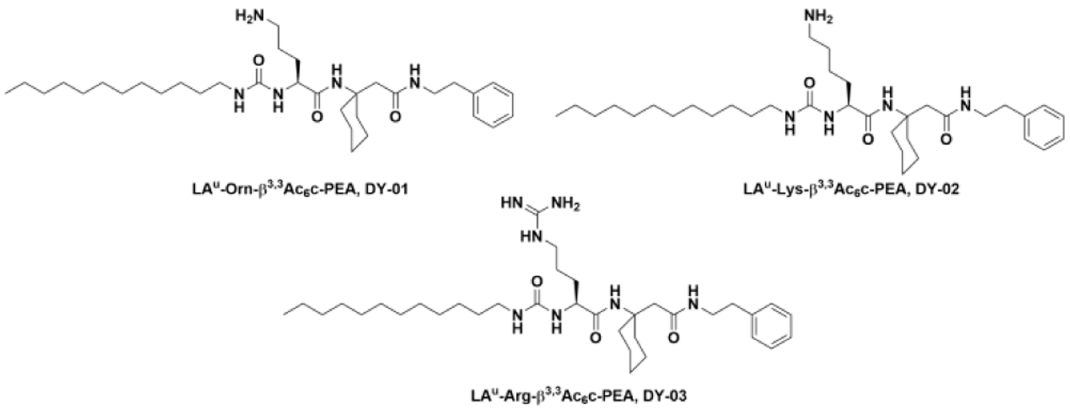

Figure 1. Chemical structures of peptides **DY-01** to **DY-03**.

Scheme 1. Synthesis of Peptides DY-01 to DY-03[a]

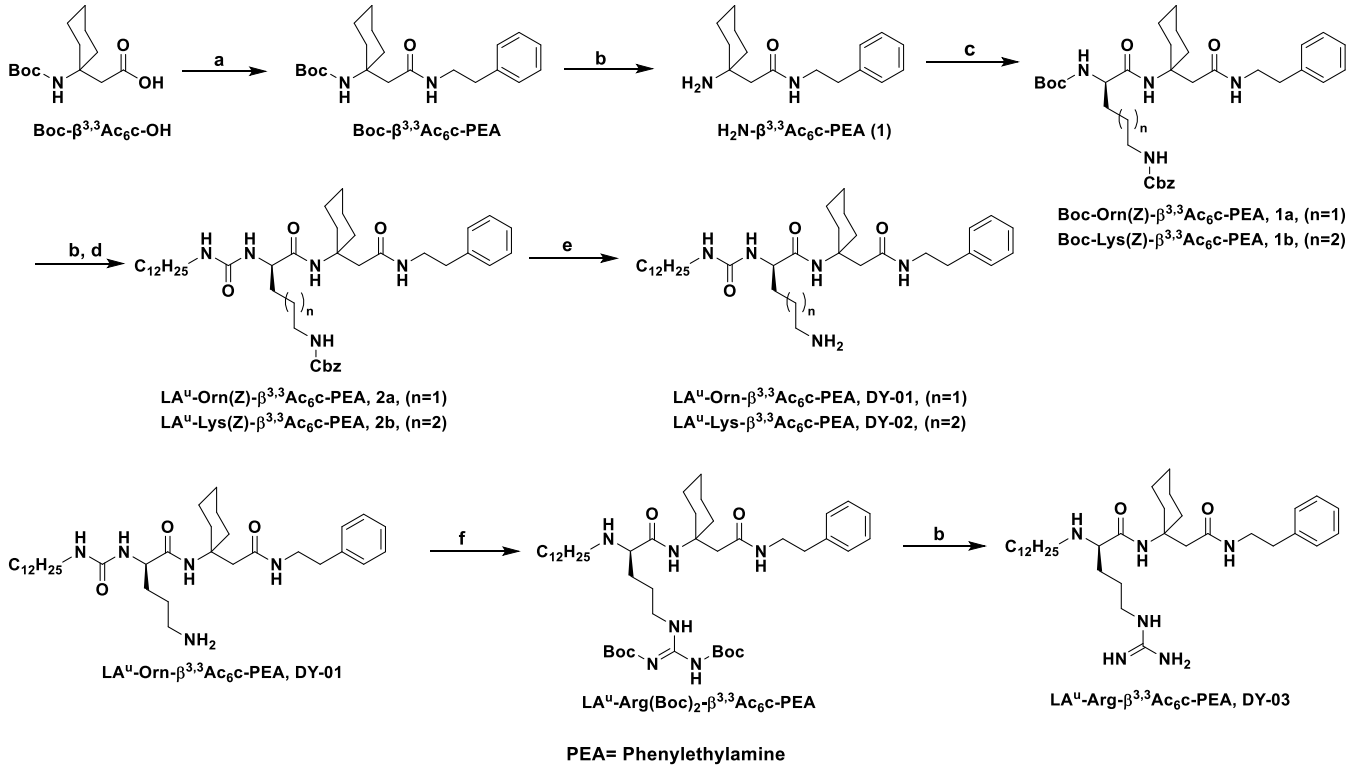

[a]Reagents and conditions: (a) Dry DCM, NMM, and EDCI·HCl, 0 °C-rt 12 h; (b) 4N-HCl in 1,4-dioxane, rt, 1 h; (c) Boc-Orn(Z)-OH/Boc-Lys(Z)-OH, dry DMF, NMM, EDCI·HCl, rt, 12 h; (d) dry DMF, NMM, dodecyl isocyanate, rt, 6 h; (e) MeOH, palladium 10% on carbon, H_2, rt, 12 h; (f) dry DMF, NMM, *N,N′*-di-Boc-1*H*-pyrazole-1-carboxamidine, rt, 8 h.

synthetic peptides are designed with amino acid sequences similar to naturally occurring AMPs that include desired modifications to enhance their efficacy.[7] Their diverse structures and broad-spectrum activity make AMPs valuable for targeting Gram-positive and Gram-negative bacteria. Chemical modifications to AMPs, such as lipidation or peptide conjugation, have further enhanced their stability, potency, and selectivity, paving the way for them to address the clinical challenges posed by multidrug-resistant pathogens. Thus, AMPs represent a promising class of agents in the development of next-generation antimicrobials.[6]

Despite the substantial progress in developing synthetic AMPs, several challenges persist in addressing key limitations, such as short in vivo half-lives, low proteolytic stability, and high cytotoxicity.[8] These limitations hinder the establishment of AMPs as efficient therapeutic agents suitable for clinical application.[8] To overcome these limitations, various strategies have been employed to AMPs, including the incorporation of unnatural amino acids,[9,10] the replacement of amide bonds with bioisosteres, and peptide cyclization. Lipidation of AMPs has also emerged as a powerful modification that can significantly enhance their therapeutic potential. This modification often improves the stability, activity, and selectivity of AMPs, particularly in serum environments, by increasing their affinity for bacterial membranes while helping to evade rapid clearance by the kidneys and liver.[11] In particular, lipidated forms of peptides can expand the antimicrobial spectrum to include both Gram-positive and Gram-negative pathogens,

https://doi.org/10.1021/acsomega.4c08680
ACS Omega 2025, 10, 2102−2115

even enabling activity in species typically resistant to nonlipidated AMPs. The addition of lipid chains, such as C12 or C14 fatty acids, tends to enhance the peptide's interaction with bacterial cell membranes, often by promoting membrane permeabilization, a key mechanism for rapid bactericidal action. Studies also highlight that lipidation reduces the risk of bacterial resistance development due to its nonspecific membrane-targeting mode of action, making these peptides valuable candidates against multidrug-resistant strains.[12,13] However, the choice of lipid chain length and placement is crucial as it can also influence cytotoxicity, underscoring the importance of optimizing lipid−AMP combinations to achieve maximal efficacy with minimal host cell toxicity. Replacing the amide bond in peptides with a urea bond is also a promising strategy to enhance the pharmacokinetic and pharmacodynamic properties. This modification has been shown to improve stability, extending half-life and enhancing bioavailability.[14−16] It has also been previously reported that the peptides with urea bonds are more potent drugs in comparison to the peptides with amide bonds,[17−21] increasing the notable antibacterial activities by connecting to C12 alkyl chains through urea linkage than amide linkage.[22]

Based on our earlier reports, we have endeavored to synthesize lipidated ureido derivatives of the previously reported short α/β cationic peptides,[22,23] LA^{U}-Orn-$\beta^{3,3}$Ac$_6$c-PEA, **DY-01**; LA^{U}-Lys-$\beta^{3,3}$Ac$_6$c-PEA, **DY-02**; and LA^{U}-Arg-$\beta^{3,3}$Ac$_6$c-PEA, **DY-03**. The chemical structures of the peptides **DY-01** to **DY-03** are shown in Figure 1. All of the synthesized peptides were comprehensively evaluated against Gram-negative and Gram-positive WHO-priority pathogens to explore their effectiveness in combating MDR pathogen-associated infections.

RESULTS

Peptide Synthesis and Characterization. The β,β di-substituted $\beta^{3,3}$Ac$_6$c was synthesized according to the procedure reported in the literature.[23,24] The peptides **DY-01** to **DY-03** were synthesized in the solution phase (Scheme 1) and characterized using an NMR (Figures S4−S6) and high-resolution mass spectra (HRMS) (Figures S7−S9) spectrophotometer. All the peptides are ≥95% pure by RP-HPLC analysis (Figures S1−S3).

Antibacterial Susceptibility Assays of the Peptides. Table 1 presents the minimal inhibitory concentration (MIC) and minimal bactericidal concentration (MBC) values of peptides **DY-01** to **DY-03** against *Pseudomonas aeruginosa* and methicillin-resistant *Staphylococcus aureus* (MRSA). **DY-01** demonstrated significant antimicrobial activity against *P. aeruginosa* and MRSA with a MIC of 2.5 μM. Peptides **DY-02** and **DY-03** showed MIC values of 5 μM against *P. aeruginosa* and 2.5 μM against MRSA. The reference antibiotics rifampicin (MIC of 0.9 μM) and vancomycin (MIC of 3.1 μM) were used in the study. Comparison of the concentration-dependent growth inhibition against *Pseudomonas* and MRSA by the peptides **DY-01** to **DY-03** depicted in Figure 2A,B indicated significant and effective antimicrobial activity. The MBC values for the peptides against the specified bacterial species were found to be the same as the MIC values, as shown in Table 1 and Figure 2C−H. Table 2 shows the MIC values of peptides ranging from 3.1 to 6.25 μM against MDR clinical isolates of *P. aeruginosa*, whereas Table 3 details the MIC values of peptides against MDR clinical isolates of *S. aureus* ranging from 0.78 to 6.25 μM. These assays suggested peptides **DY-01** to **DY-03** have significant broad-spectrum bactericidal efficacy against MDR-bacterial strains.

Table 1. MIC and MBC Values of the Peptides against *P. aeruginosa* and MRSA

	MIC (μM)		MBC (μM)	
Peptides	*P. aeruginosa*	MRSA	*P. aeruginosa*	MRSA
DY-01	2.5	2.5	2.5	2.5
DY-02	5	2.5	5	2.5
DY-03	5	2.5	5	2.5
rifampicin	0.9			
vancomycin		3.1		

Time-Kill Kinetics. The time-kill assay was conducted to evaluate the time-dependent bactericidal activity of peptides **DY-01** to **DY-03** against *P. aeruginosa* and MRSA. The results are graphically represented in Figure 3A,B, respective for *Pseudomonas* and MRSA. Figure 3A demonstrates the bactericidal activity of **DY-01**, **DY-02**, and **DY-03** against *P. aeruginosa* compared to that of the untreated control. For **DY-01**-treated cells, the *pseudomonal* population declined significantly, with complete eradication observed by the sixth hour. The bactericidal effect was evident, with a complete decline in bacterial population by the fifth hour for **DY-02**, whereas **DY-03** showed a gradual decline, achieving complete bactericidal activity by the sixth hour. Figure 3B depicts the bactericidal activity of the peptides against MRSA. **DY-01** and **DY-02** showed complete bactericidal activity, eliminating the bacterial population by the sixth hour. **DY-03** demonstrated the fastest bactericidal effect, with complete eradication observed by the third hour.

Antibiofilm and Swarming Inhibition by the Peptides. This experiment evaluated the antibiofilm efficacy of peptides **DY-01**, **DY-02**, and **DY-03** in a concentration-dependent manner against *P. aeruginosa* and MRSA biofilm. The peptides **DY-01** and **DY-02** inhibited pseudomonal biofilm formation by ∼1.0−2 times at 2 × MIC than the untreated samples (Figure 3C), escalating to a 4 times inhibition at 4 × MIC. These peptides similarly affected MRSA biofilm formation in a concentration-dependent manner (Figure 3E). Furthermore, the peptides were tested against the preformed *pseudomonal* and MRSA biofilm, and biofilm disruption by the peptides is presented in Figure 3D,F. The peptides effectively disrupt established biofilm of *P. aeruginosa* by ∼1−3 times at 2 × MIC and 4 × MIC, respectively. Against MRSA, the peptides achieved ∼1.0−1.5 times disruption at MIC and 2 × MIC, escalating to a 2 times disruption at 4 × MIC.

The swarming motility inhibition by the peptides is depicted in Figure 6. In the medium control (no growth), Figure 6A and the untreated sample (Figure 6B) of *P. aeruginosa* exhibited distinct dendritic pattern motility. In contrast, the rifampicin-treated control (Figure 6C) showed a whirl-like motion with reduced motility, whereas Figure 6D−F demonstrates that peptides **DY-01**, **DY-02**, and **DY-03** significantly inhibited the swarming motility of *P. aeruginosa* as no motility was noticed. The experiment was not extended to MRSA due to its nonswarming behavior.

Synergistic Potential of Peptides with Rifampicin and Vancomycin. Antimicrobial synergy is crucial for enhancing the efficacy of antimicrobial agents, while reducing resistance

https://doi.org/10.1021/acsomega.4c08680
ACS Omega 2025, 10, 2102−2115

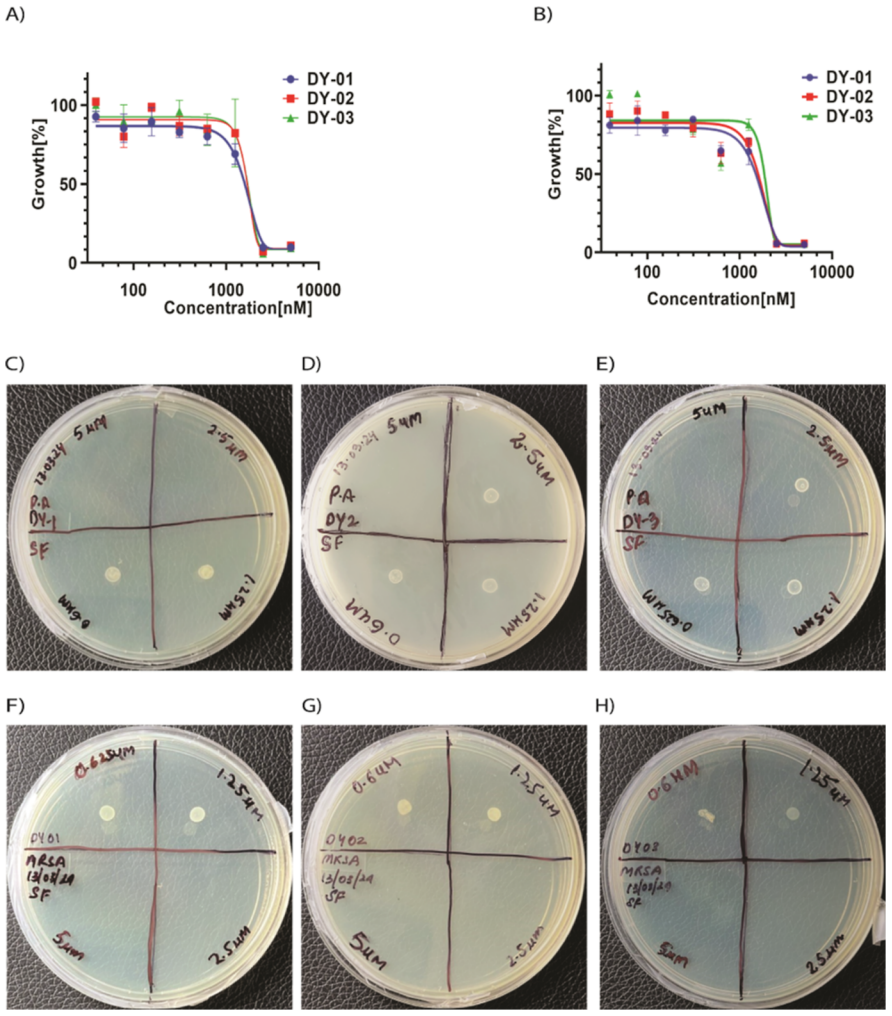

Figure 2. Antimicrobial activity of the short $\alpha\beta$ cationic peptides. (A,B) Graphical representation of concentration-dependent growth inhibition of *P. aeruginosa* and MRSA by **DY-01**, **DY-02**, and **DY-03**. (C−H) MBC of (C) **DY-01**, (D) **DY-02**, (E) **DY-03** against *P. aeruginosa*, (F) **DY-01**, (G) **DY-02**, and (H) **DY-03** against MRSA.

Table 2. MIC of the Peptides against MDR *P. aeruginosa* Clinical Isolates

P. aeruginosa clinical isolates	DY-01 (μM)	DY-02 (μM)	DY-03 (μM)	rifampicin (μM)
PA-76	3.1	6.25	3.1	6.25
PA-78	3.1	6.25	3.1	25
PA-81	3.1	6.25	3.1	0.62
PA-87	6.25	6.25	3.1	25
PA-95	3.1	6.25	3.1	25
PA-MTCC 424	3.1	6.25	3.1	0.62

Table 3. MIC of the Peptides against MDR *S. aureus* Clinical Isolates

S. aureus clinical isolates	DY-01 (μM)	DY-02 (μM)	DY-03 (μM)	vancomycin (μM)
SA-310	0.78	3.12	1.56	50
SA-306	0.78	1.56	1.56	0.78
SA-346	1.56	3.12	6.25	25
SA-345	0.78	3.12	3.12	25
SA-318	0.78	3.12	3.12	12.5
MRSA	2.5	2.5	2.5	3.1

development. This assay examined 77 combinations of peptides (**DY-01**, **DY-02**, and **DY-03**) and standard antibiotics (rifampicin and vancomycin) against *P. aeruginosa* and MRSA, respectively (Figure 4). Additionally, the FICI values were calculated. This assay yielded 5, 11, and 5 synergistic interactions between rifampicin and peptides against *P. aeruginosa*, with a substantial decrease in MIC values for both the peptide and the antibiotic (**DY-01**: 2.5 μM up to 0.15 μM; rifampicin: 0.9 μM up to 0.07 μM; **DY-02**: 5 μM up to 0.07 μM; rifampicin: 0.9 μM up to 0.004 μM; **DY-03**: 5 μM up to 0.004 μM; rifampicin: 0.9 μM up to 0.15 μM) (Figure 4A−C). Furthermore, 15, 10, and 10 synergistic interactions were found between vancomycin and peptides against MRSA, with a significant decrease in MIC values for both the peptide and the antibiotic (**DY-01**: 2.5 μM up to 0.07 μM; vancomycin: 3.1 μM up to 0.01 μM; **DY-02**: 2.5 μM up to 0.07 μM; vancomycin: 3.1 μM up to 0.31 μM; **DY-03**: 2.5 μM up to 0.07 μM; vancomycin: 3.1 μM up to 0.15 μM) (Figure 4D−F). The synergy values are incorporated in the Supporting Information, Table S1.

Scanning Electron Microscopic Investigations with the Peptide-Treated Cells. Scanning electron microscopy (SEM) analysis was conducted on *P. aeruginosa* and MRSA, to visualize the morphological changes in the peptide-treated and

https://doi.org/10.1021/acsomega.4c08680
ACS Omega 2025, 10, 2102−2115

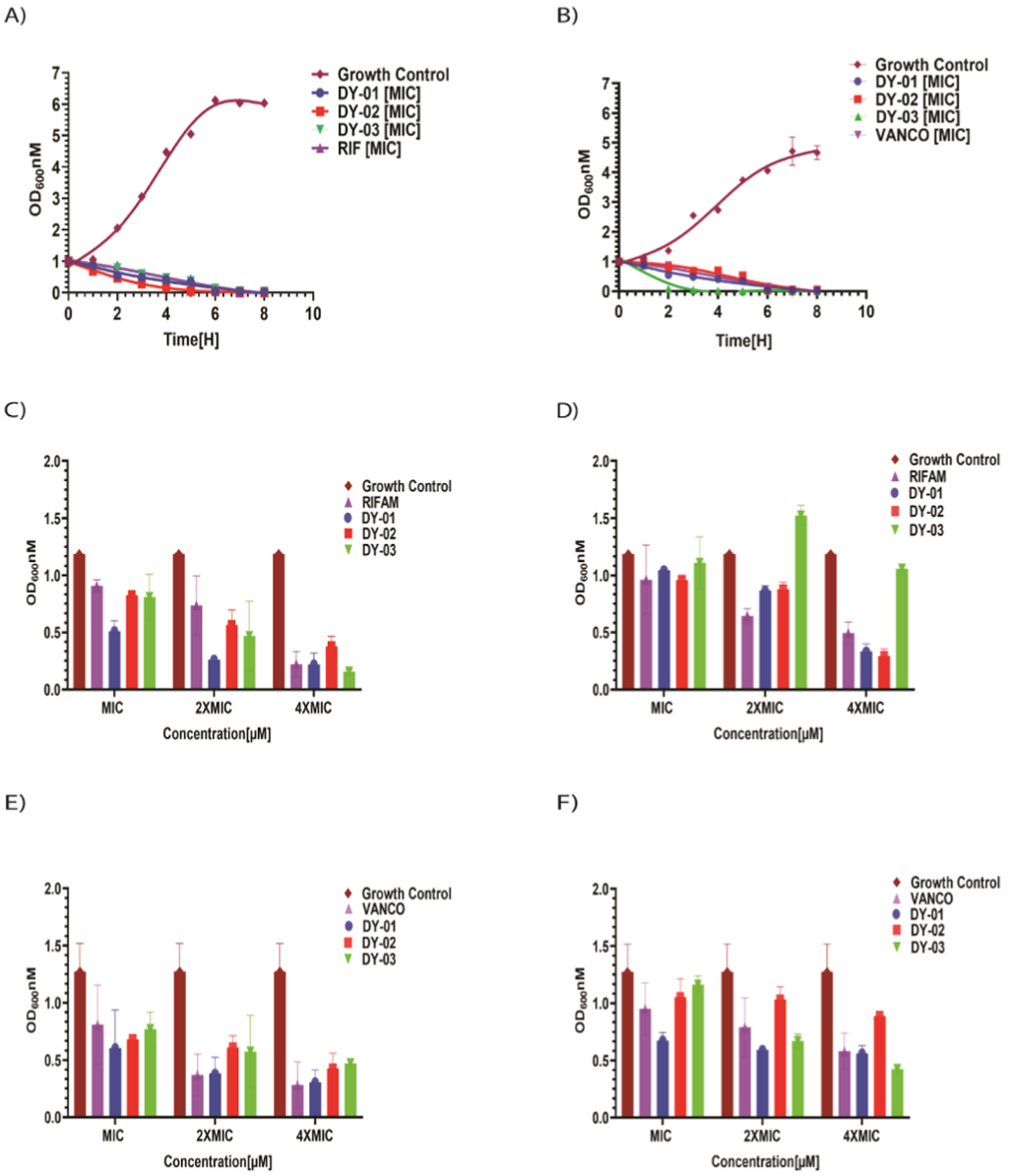

Figure 3. Time-kill kinetics and antibiofilm efficacy of the short $\alpha\beta$ cationic peptides. (A) Time-kill assay of **DY-01**, **DY-02**, and **DY-03** at MIC concentration represented against *P. aeruginosa* comparable to standard drug control rifampicin. (B) Time-kill assay of **DY-01**, **DY-02**, and **DY-03** at MIC concentration represented against MRSA comparable to standard drug control vancomycin. (C,D) Biofilm inhibition and disruption at MIC, 2 × MIC, and 4 × MIC concentrations of **DY-01**, **DY-02**, **DY-03**, and standard drug control rifampicin against *P. aeruginosa*. (E,F) Biofilm inhibition and disruption at MIC, 2 × MIC, and 4 × MIC concentrations of **DY-01**, **DY-02**, **DY-03**, and standard drug control vancomycin against MRSA.

untreated cells. Figure 5A−H depicts the effects of **DY-01**, **DY-02**, and **DY-03** treatment on *P. aeruginosa* cells, while Figure 5I−P shows the morphological changes in *staphylococcal* cells treated with these peptides. For *P. aeruginosa*, the untreated growth control (Figure 5A,E) displayed smooth-surfaced, rod-shaped cells without any abnormalities. In contrast, peptide-treated cells exhibited rough, irregular patterns and significant elongation and disruption, indicating impaired cell division followed by lysis (**DY-01**: Figure 5B,F; **DY-02**: Figure 5C,G; **DY-03**: Figure 5D,H). These morphological alterations suggest that the peptides disrupt the bacterial membrane and affect the normal cell cycle of *P. aeruginosa*. For MRSA, the untreated growth control (Figure 5I,M) showed a typical spherical, grape-like structure, whereas the peptide-treated cells displayed damaged cell walls and leakage of cellular components (**DY-01**: Figure 5J,N; **DY-02**: Figure 5K,O; **DY-03**: Figure 5L,P). These observations indicate that the peptides significantly compromise the cell membrane integrity, leading to increased bacterial apoptosis in MRSA.

Ex Vivo Efficacy of Peptides. The cell infection model experiment demonstrated the effectiveness of peptides **DY-01**, **DY-02**, and **DY-03** in treating internalized bacterial populations in A549 human type II alveolar epithelial cells. For *Pseudomonas*, the untreated control cells showed a significant increase in the bacterial population with respect to the initial bacterial population over time. Comparatively, the peptide-treated samples exhibited a decrease in bacterial population after treatment with peptides (Figure 7A,B). For **DY-01**, the bacterial population decreased nearly 2, 3, and 4 times at MIC, 2 × MIC, and 4 × MIC concentrations,

https://doi.org/10.1021/acsomega.4c08680
ACS Omega 2025, 10, 2102−2115

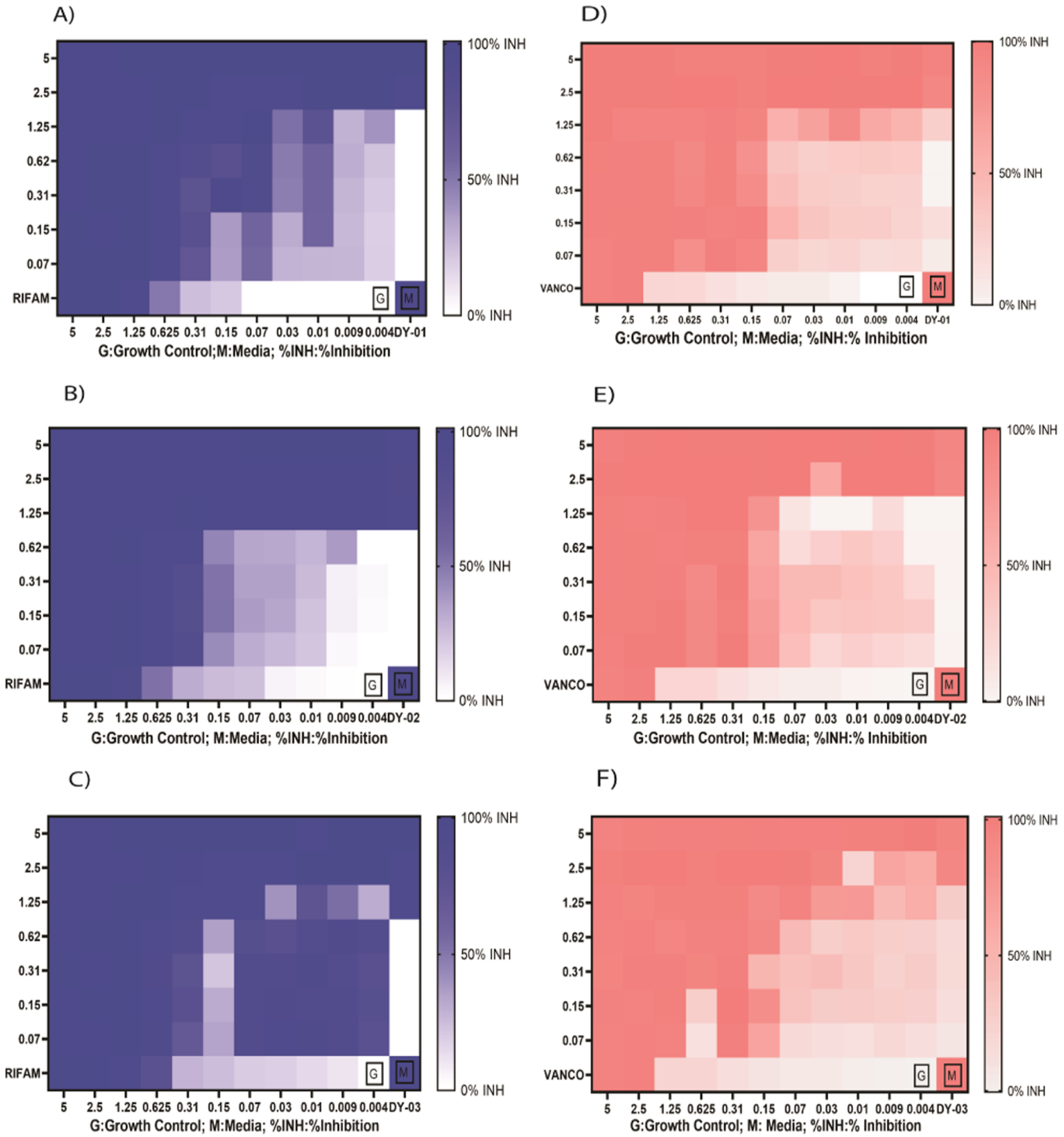

Figure 4. Checkerboard assay determining synergistic potential of the short $\alpha\beta$ cationic peptides. (A) Heat map of **DY-01** with rifampicin, (B) **DY-02** with rifampicin, and (C) **DY-03** with rifampicin against *P. aeruginosa* (dark-blue color represents complete growth inhibition, whereas no color represents bacterial growth). (D) Heat map of **DY-01** with vancomycin, (E) **DY-02** with vancomycin, and (F) **DY-03** with vancomycin against MRSA (dark-pink color represents complete growth inhibition, whereas no color represents bacterial growth).

respectively. For **DY-02**, the *pseudomonal* population decreased ~2 times at MIC and 2 × MIC concentrations; at 4 × MIC, a plateau was reached, indicating no further significant reduction. Notable reduction of CFU was also observed in **DY-03**-treated samples (Figure 7A). In MRSA-infected cells, the treated samples showed a significant decrease in bacterial population with the increasing concentration of the peptides, whereas the untreated control cells showed an increase in bacterial population over time (Figure 7B). This experiment underscores the potential of peptides **DY-01**, **DY-02**, and **DY-03** in combating *P. aeruginosa* and MRSA infections, mimicking natural tissue conditions with minimal modifications.

In Vitro Cytotoxicity Analysis of the Peptides. The cytotoxicity of peptides **DY-01**, **DY-02**, and **DY-03** was evaluated on two different cell lines, RAW 264.7 and J774A.1, as shown in Figure 8A,B. The cell viability of the

https://doi.org/10.1021/acsomega.4c08680
ACS Omega 2025, 10, 2102−2115

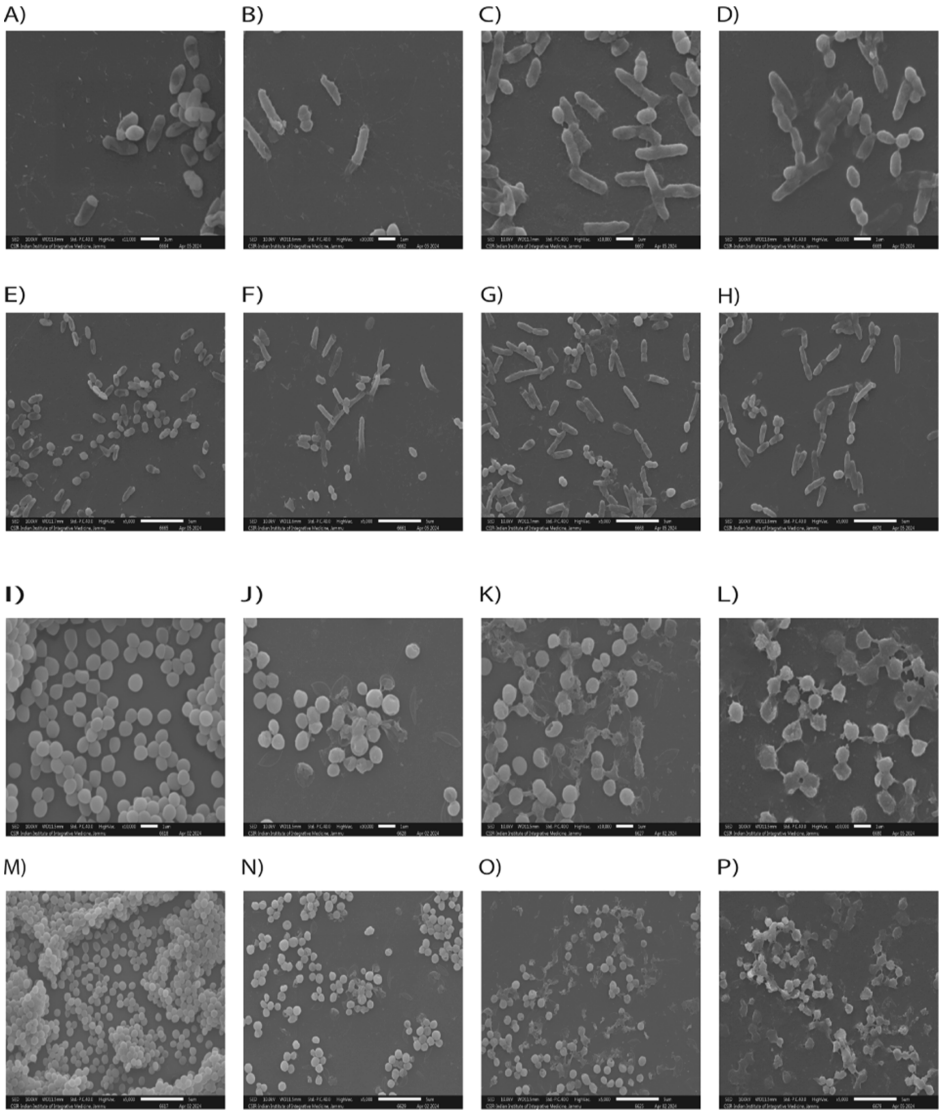

Figure 5. Ultrastructure images examined under the scanning electron microscope. The images are captured at two magnifications (11,000× and 5000×), with lower magnification showing high cell density and vice versa. The upper panel shows various images of *P. aeruginosa*: (A,E) untreated samples, (B,F) **DY-01**-treated, (C,G) **DY-02**-treated, and (D,H) **DY-03**-treated at the magnifications mentioned above. The lower panel shows various images of MRSA: (I,M) untreated samples, (J,N) **DY-01**-treated, (K,O) **DY-02**-treated, and (L,P) **DY-03**-treated at the magnifications mentioned above.

growth control (100%) was compared to that of peptides at different concentrations. For the RAW 264.7 cell line (Figure 8A), no toxicity was observed at 10 μM, and good cell viability was maintained. At 20 μM, the peptides showed mild toxicity with varying degrees of cell survival. For the J774A.1 cell line (Figure 8B), cell viability at 10 μM was comparable to that of the growth control. At 20 μM, **DY-01** exhibited a substantial decline in cell viability, while **DY-02** and **DY-03** had no major impact on cell viability. Furthermore, the hemolysis assay was conducted to assess the potential of these peptides to cause lysis of erythrocytes in blood (Figure 8C). Triton-X 100 (1%) was used as a positive control, completely lysing the erythrocytes (100%), and PBS was a negative control. At 20 μM, peptides caused 80% lysis compared to Triton-X 100. At 10 μM, **DY-01** caused 70% lysis, while **DY-02** and **DY-03** caused 30% lysis. At 5 μM, all peptides caused significantly less lysis than those at higher concentrations. Overall, the cytotoxicity assays indicated that **DY-01**, **DY-02**, and **DY-03** have varying impacts on cell viability depending on the cell line and concentration used. The selectivity indexes of the peptides against different cell lines are shown in Table 4.

DISCUSSION

AMR in bacteria is a significant public health concern in the 21st century.[25] The rise and spread of MDR pathogens, particularly *P. aeruginosa* and MRSA, represent a serious global threat. These pathogens are notorious for their resistance to multiple antibiotics, making infections challenging to treat. The pressing need for new therapeutic agents and alternative treatment strategies to combat these drug-resistant infections cannot be overstated. In this context, AMPs have garnered attention due to their remarkable effectiveness against MDR pathogens. However, the clinical application of AMPs has been hindered by several challenges, including potential toxicity to host cells, instability under physiological conditions, vulnerability to enzymatic degradation, and high production costs due to their complex structures.[26] The development of ultrashort cationic hybrid AMPs might overcome the

https://doi.org/10.1021/acsomega.4c08680
ACS Omega 2025, 10, 2102−2115

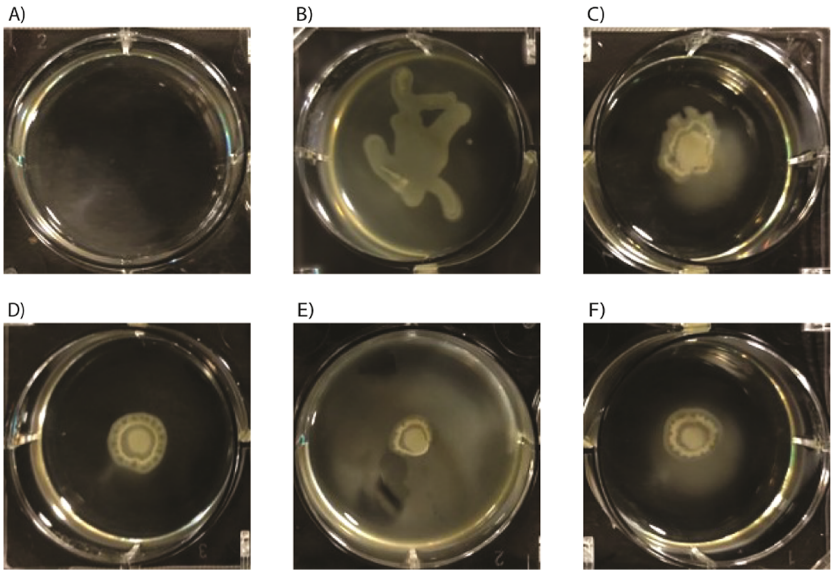

Figure 6. Swarming motility assay of *P. aeruginosa* on a 0.5% agar medium. (A) Media control, (B) growth control, (C) sub-MIC-added rifampicin (standard antibiotic control), (D) sub-MIC-added **DY-01**, (E) sub-MIC-added **DY-02**, and (F) sub-MIC-added **DY-03**.

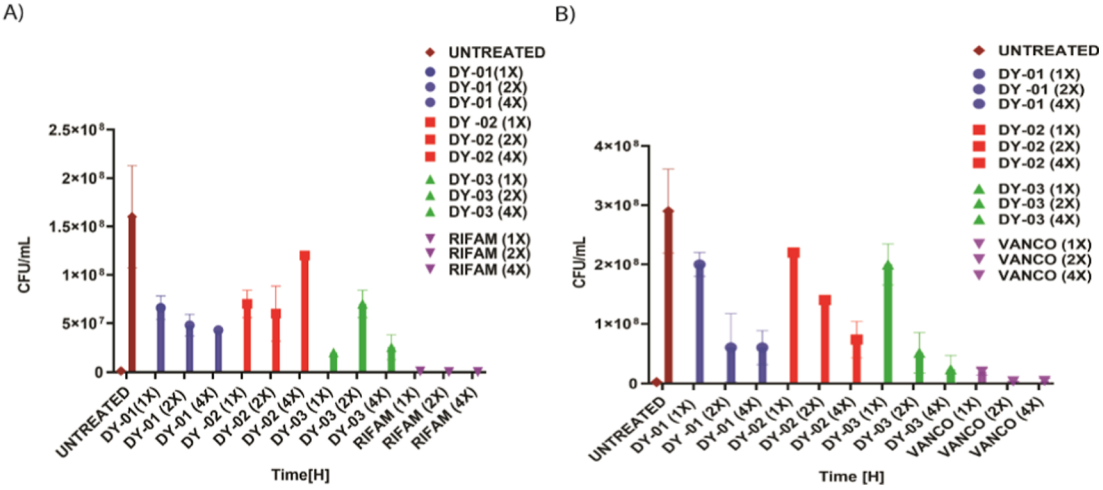

Figure 7. Ex vivo infection model on the A549 cell line. The ex vivo infection of (A) *P. aeruginosa* and (B) MRSA on the A549 cell line treated with peptides **DY-01**, **DY-02**, and **DY-03** along with standard antibiotics rifampicin and vancomycin.

challenges associated with AMPs.[27,28] Our study focuses on a series of short $\alpha\beta$ cationic peptides (**DY-01** to **DY-03**), which were synthesized based on our previously reported peptide LA-Lys-$\beta^{3,3}$Ac$_6$c-PEA, P4.[22] $\alpha\beta$ Hybrid peptides represent a promising class of antibacterial compounds with significant potential in drug discovery. Their unique structure, combining α-amino acids and β-amino acids, offers enhanced proteolytic stability, which is a key challenge in peptide-based therapeutics.[29] The inclusion of β-amino acids not only improves the peptide's resistance to enzymatic degradation but also enables the fine-tuning of physicochemical properties, such as hydrophobicity and charge distribution, which are crucial for antibacterial activity.[30] These peptides were designed with novel modifications of the original P4 structure. Specifically, urea was introduced in place of the amide bond. In **DY-01** to **DY-03**, the C12 lipid chain is conjugated at the N terminus of the peptide through urea bonds to enhance the activity with less cytotoxicity. The design and synthesis of these peptides were aimed to enhance stability, half-life, and efficacy as urea-containing compounds are well-known in medicinal chemistry and drug design for their capacity to form essential drug−target interactions and enhance important drug-like properties.[15]

Our antibacterial efficacy assays demonstrated broad-spectrum antibacterial efficacy against *P. aeruginosa* and MRSA. **DY-01** showed the most potent activity, with an MIC of 2.5 μM for both pathogens. **DY-02** and **DY-03** also displayed notable efficacy, particularly against MRSA with MIC values of 2.5 μM. Additionally, these peptides showed bactericidal potency against MDR clinical isolates of *P. aeruginosa* and MRSA. **DY-01** and **DY-03**, in particular, maintained low MIC values across various strains, highlighting their robustness against resistant pathogens, whereas the original peptide P4 has shown MIC and MBC values of 6.25 and 12.5 μM, respectively, for *P. aeruginosa*. In contrast, it showed MIC and MBC values of 25 μM and 50 μM, respectively, for MRSA.[22] The presently synthesized peptides have shown better efficacy than the original peptide P4. Most interestingly, these peptides retained their efficacy against the MDR clinical isolates of these pathogens, suggesting their

https://doi.org/10.1021/acsomega.4c08680
ACS Omega 2025, 10, 2102−2115

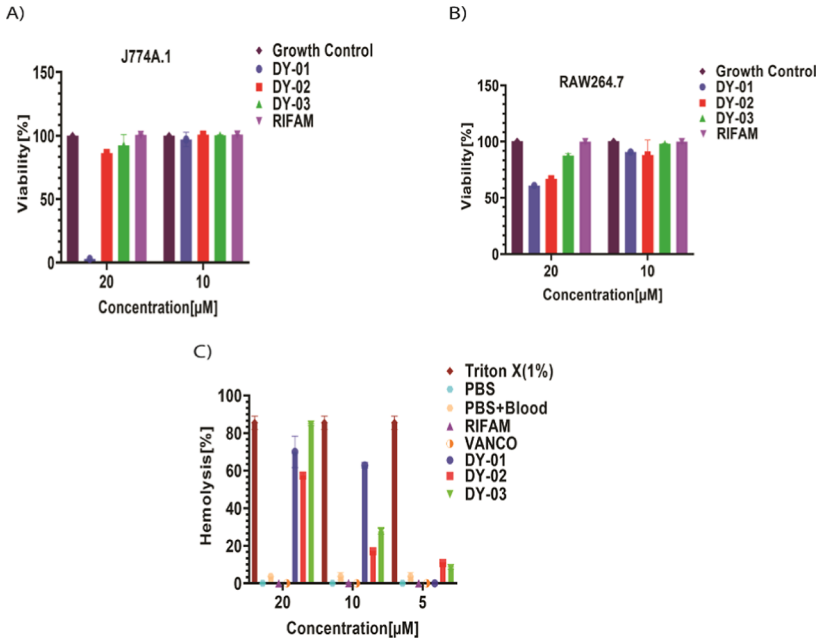

Figure 8. MTT cytotoxicity and hemolysis assay analysis. The cell viability of (A) J774A.1 cell line and (B) RAW264.7 cell line treated with peptides **DY-01**, **DY-02**, and **DY-03** and rifampicin. (C) Percentage hemolysis of red blood cells compared to positive control, Triton X-100.

Table 4. Selectivity Index of the Peptides for Cytotoxicity and Hemolysis Assay[a]

	Selectivity index		
Peptides	RAW 264.7	J774A.1	hemolysis
DY-01	8.1	4.3	0.2
DY-02	10.1	8.7	8.2
DY-03	7.0	8.9	5.1

[a]For calculating selectivity index, an MIC value of 2.5 μM is considered.

potency in combating chronic and resistant infections. Altogether, we suggest that the modifications in peptide P4 have significantly increased its efficacy against *P. aeruginosa* and MRSA.

Inhibition or disruption of bacterial biofilm formation is a crucial parameter in antibacterial drug discovery, as biofilms provide increased resistance to antimicrobial drugs.[31] The two nosocomial pathogens *P. aeruginosa* and MRSA are known for their biofilm-forming capabilities. Our study demonstrated that **DY-01**, **DY-02**, and **DY-03** effectively inhibit and disrupt biofilms of *P. aeruginosa* and MRSA. This ability to target biofilms enhances their therapeutic potential, particularly for chronic and device-associated infections. This inhibition of *pseudomonal* motility suggests that these peptides can effectively limit bacterial dissemination and colonization, further supporting their antimicrobial potential. Combining AMPs with conventional antibiotics can enhance efficacy and reduce resistance.[32,33] Our checkerboard assays revealed several synergistic interactions between the peptides with rifampicin and vancomycin against *P. aeruginosa* and MRSA, respectively, at lower concentrations. These interactions suggest that combining these peptides with existing antibiotics could improve treatment outcomes and reduce the likelihood of resistance development.[32−34] The observed combinational efficacy at lower concentrations between rifampicin and the peptides may be attributed to their different mechanisms of action against *Pseudomonas*. The synergistic interaction between vancomycin and the peptides could result from the combined membrane-permeabilization action of vancomycin and the peptides, leading to increased penetration into bacterial cells and augmented killing.[35,36] Peptide-treated *P. aeruginosa* cells exhibited significant morphological changes, including rough, irregular surfaces and cell elongation, indicating disrupted cell division and membrane integrity. MRSA cells treated with peptides showed damaged membranes, disrupted cell walls, and leakage of cellular contents. These morphological alterations confirm that the peptides compromise the bacterial membrane integrity, leading to cell death. Furthermore, we demonstrated that peptides **DY-01**, **DY-02**, and **DY-03** significantly reduced bacterial load in an A549 human type II alveolar epithelial cell infection model, indicating that these peptides can penetrate mammalian cells without causing damage while retaining their bactericidal effect inside the host cell. These findings underscore the potential of these peptides as antimicrobial agents. Safety is a critical consideration in the development of antimicrobial agents. Our cytotoxicity assays on RAW 264.7 and J774A.1 cell lines indicated that **DY-01**, **DY-02**, and **DY-03** exhibit minimal cytotoxicity at lower concentrations, with some cytotoxic effects observed at higher doses. Hemolysis assays revealed that the peptides caused significant erythrocyte lysis at higher concentrations but were much safer at lower doses. The balance between effective antimicrobial activity and minimal cytotoxicity and hemolytic activity is crucial for their application in treating microbial infections. **DY-02** and **DY-03**, in particular, appear to offer a promising therapeutic window, combining potent antimicrobial properties with lower cytotoxic and hemolytic effects, making them strong candidates for further development as antimicrobial agents.

CONCLUSIONS

Our comprehensive antibacterial efficacy analysis of peptides **DY-01**, **DY-02**, and **DY-03** against *P. aeruginosa* and MRSA

https://doi.org/10.1021/acsomega.4c08680
ACS Omega 2025, 10, 2102−2115

reveals their significant potential as antimicrobial agents. Cytotoxicity and hemolysis assays suggest the need for further optimization of the peptides. Overall findings underscore the importance of urea in place of the amide bond in **DY-01** to **DY-03**, which provides a strong rationale for further development and optimization of the peptides for potential clinical application in combating microbial infections, particularly those involving biofilms and resistant strains.

MATERIALS AND METHODS

Chemistry. All of the chemicals and reagents were purchased from commercial vendors Sigma-Aldrich, Novabiochem, TCI Chemicals, Avra Synthesis, Spectrochem, and HiMedia, India, and were used without purification. The peptides **DY-01** to **DY-03** were synthesized in the solution phase and the reaction mixtures were monitored using thin-layer chromatography on 0.25 mm silica gel 60 F_{254} plates coated on an aluminum sheet. The peptides were purified by normal column chromatography using silica gel 100−200 mesh as the stationary phase, and $CHCl_3/CH_3OH$ was used as the mobile phase. The purity was determined by using RP-HPLC (Agilent Technologies 1200 series) with a linear gradient of 85−100% acetonitrile in water, containing 0.01% TFA for 15 min in a reversed-phase C18 analytical column (4.6 × 25 mm, particle size 5.0 μm) at a flow rate of 1.0 mL/min. The ^{1}H NMR spectra were recorded on Bruker DPX-400 using dimethyl sulfoxide DMSO-d_6 as the solvent with TMS as the internal standard. The HRMS were recorded on a Waters XEVO-G2-XS-Q-TOF mass spectrometer.

Peptide Synthesis (DY-01 to DY-03). *Synthesis of H_2N-$\beta^{3,3}$-Ac_6c-PEA, **1**.* To a solution of Boc-$\beta^{3,3}Ac_6c$−OH (1.2 g, 5.0 mmol) in dry DCM, NMM (1.5 mL, 15.0 mmol), EDC·HCl (1.146 g, 6.0 mmol), and phenylethylamine (1.364 g, 6 mmol) were added at 0 °C. The reaction mixture was allowed to attain room temperature and stirred for 12 h. Upon completion, the solvent was evaporated, and the crude residue was extracted with water and ethyl acetate (3 × 25 mL). The ethyl acetate layers were combined and washed with 2 N-HCl (1 × 20 mL), 2 N-$NaHCO_3$ (1 × 20 mL), and saturated brine solution (1 × 20 mL) and dried over anhydrous Na_2SO_4. The organic layer was evaporated under vacuum to obtain Boc-$\beta^{3,3}Ac_6c$-PEA. The *tert*-butyloxycarbonyl group of Boc-$\beta^{3,3}Ac_6c$-PEA was deprotected using 5 mL of 4 N-HCl in 1,4-dioxane and stirred for 1 h at room temperature. Upon completion, the solvent was evaporated to afford H_2N-$\beta^{3,3}Ac_6c$-PEA, **1** (yield 91%, 1.5 g), which was used further without purification.

*Synthesis of LA^U-Orn-$\beta^{3,3}Ac_6c$-PEA, **DY-01**.* Boc-Orn(Z)-OH (2.3 g, 6.48 mmol) was dissolved in 4 mL of dry DMF and NMM (1.6 mL, 16.2 mmol) and EDC·HCl (1.2 g, 6.48 mmol) were added at 0 °C. After 10 min, H_2N-$\beta^{3,3}Ac_6c$-PEA (1.5 g, 5.4 mmol) was added and stirred for 12 h at room temperature. Upon completion, the work up and the *tert*-butyloxycarbonyl group was deprotected following the procedure described for **1** to afford H_2N-Orn(Z)-$\beta^{3,3}Ac_6c$-PEA, **1a** which was further used without purification. To the solution of H_2N-Orn(Z)-$\beta^{3,3}Ac_6c$-PEA (0.5 g, 1.0 mmol) in dry DMF were added NMM (0.2 mL, 2.4 mmol) and dodecyl isocyanate (0.5 g, 2.4 mmol) at room temperature and stirred for 6 h. Upon completion, the work up was performed following the procedure described for **1** and the resulting residue was purified by column chromatography using 100−200 silica gel in $CHCl_3/CH_3OH$ (99:01) to obtain LA^U-Orn(Z)-$\beta^{3,3}Ac_6c$-PEA. Further, the benzyloxycarbonyl group of LA^U-Orn(Z)-$\beta^{3,3}Ac_6c$-PEA (0.450 g, 0.625 mmol) was deprotected using palladium 10% on carbon (0.033 g 0.32 mmol) in 5 mL of methanol under a H_2 atmosphere. The reaction mixture was filtered through celite and continuously washed with methanol to remove Pd/C. The filtrate was evaporated and dried under reduced pressure to afford LA^U-Orn-$\beta^{3,3}Ac_6c$-PEA, **DY-01** (yield 72% 0.415 g). ^{1}H NMR (400 MHz, DMSO-d_6, δ): 8.12 (dd, J = 8.1, 2.4 Hz, 1H), 8.00−7.88 (br, 2H), 7.43 (s, 1H), 7.33−7.27 (m, 4H), 7.22−7.18 (m, 1H), 6.20 (q, J = 5.3 Hz, 1H), 6.08 (dd, J = 8.2, 3.2 Hz, 1H), 4.90 (t, J = 7.3 Hz, 1H), 4.18−4.13 (m, 1H), 3.04−2.87 (m, 2H), 2.77 (t, J = 7.2 Hz, 2H), 2.64 (d, J = 1.6 Hz, 1H), 2.41 (d, J = 13.4 Hz, 1H), 2.19 (s, 1H), 2.04−2.00 (m, 1H), 1.65−1.54 (m, 3H), 1.48−1.37 (m, 7H), 1.32 (dd, J = 7.1, 1.5 Hz, 5H), 1.23 (s, 20H), 0.85 (td, J = 6.9, 1.4 Hz, 3H). HRMS (ESI) at m/z $[M + H]^+$ Calcd for $C_{34}H_{60}N_5O_3$ is 585.4696. Found: 586.4693.

*Synthesis of LA^U-Lys-$\beta^{3,3}Ac_6c$-PEA, **DY-02**.* Boc-Lys(Z)-OH (1.28 g, 3.36 mmol) was dissolved in 4 mL of dry DMF and NMM (0.84 mL, 8.4 mmol) and EDC·HCl (0.536 g, 2.8 mmol) were added at 0 °C. After 10 min, H_2N-$\beta^{3,3}Ac_6c$-PEA (0.82 g, 2.8 mmol) was added and stirred for 12 h at room temperature. Upon completion, the work up and the *tert*-butyloxycarbonyl group was deprotected following the procedure described for **1** to afford H_2N-Lys(Z)-$\beta^{3,3}Ac_6c$-PEA **1b**, which was further used without purification. To the solution of H_2N-Lys(Z)-$\beta^{3,3}Ac_6c$-PEA (0.424 mg, 0.76 mmol) in dry DMF, NMM (0.23 mL, 2.28 mmol) and dodecyl isocyanate (0.192 mL, 0.912 mmol) were added at room temperature, and the mixture was stirred for 6 h. Upon completion, the work up was performed following the procedure described for **1** and the resulting residue was purified by column chromatography using 100−200 silica gel in $CHCl_3/CH_3OH$ (99:01) to obtain LA^U-Lys(Z)-$\beta^{3,3}Ac_6c$-PEA. Further, the benzyloxycarbonyl group of LA^U-Lys(Z)-$\beta^{3,3}Ac_6c$-PEA (0.2 g, 0.3 mmol) was deprotected using palladium 10% on carbon (0.015 g, 0.15 mmol) in 5 mL of methanol under a H_2 atmosphere. The reaction mixture was filtered through celite and continuously washed with methanol to remove Pd/C. The filtrate was evaporated and dried under reduced pressure to afford LA^U-Lys-$\beta^{3,3}Ac_6c$-PEA, **DY-02** (yield 83.4%, 0.150 g). ^{1}H NMR (400 MHz, DMSO-d_6, δ): 8.12 (d, J = 8.1 Hz, 1H), 8.00−7.86 (br, 2H), 7.33−7.27 (m, 5H), 7.24−7.185 (m, 1H), 6.14−6.11 (m, 2H), 4.92−4.88 (m, 1H), 4.05 (td, J = 8.0, 4.7 Hz, 1H), 3.04−2.87 (m, 2H), 2.73 (t, J = 7.6 Hz, 2H), 2.66 (d, J = 13.4 Hz, 1H), 2.39 (d, J = 13.4 Hz, 1H), 2.30−2.20 (m, 1H), 2.02−1.98 (m, 1H), 1.62−1.50 (m, 3H), 1.47−1.35 (m, 8H), 1.32 (d, J = 7.0 Hz, 6H), 1.23 (s, 20H), 0.85 (td, J = 6.9, 1.4 Hz, 3H). HRMS (ESI) at m/z $[M + H]^+$ Calcd for $C_{35}H_{62}N_5O_3$ is 600.4853. Found: 600.4875.

*Synthesis of LA^U-Arg-$\beta^{3,3}Ac_6c$-PEA, **DY-03**.* To the solution of **DY-02** (0.227 g, 0.39 mmol) in 3 mL of dry DMF, NMM (0.12 mL, 1.17 mmol) and *N,N′*-bis[tertbutylcarbonyl]-1*H*-pyrazole-1-carboxamidine (0.145 g, 0.468 mmol) were added at room temperature and stirred for 8 h. Upon completion, the work up was performed following the procedure described for **1** and the resulting residue was purified by column chromatography using 100−200 silica gel in $CHCl_3/CH_3OH$ (99:01) to obtain LA^U-Arg-$(Boc)_2$-$\beta^{3,3}Ac_6c$-PEA. Further, the *tert*-butyloxycarbonyl group of LA^U-Arg-$(Boc)_2$-$\beta^{3,3}Ac_6c$-PEA (0.1 g, 0.17 mmol) was deprotected following the procedure described for **1** to afford LA^U-Arg-$\beta^{3,3}Ac_6c$-PEA, **DY-03** (yield 72%, 0.096.g). ^{1}H NMR (400 MHz, DMSO-d_6, δ): 8.10 (d, J =

https://doi.org/10.1021/acsomega.4c08680
ACS Omega 2025, 10, 2102−2115

8.1 Hz, 1H), 7.61 (d, J = 18.3 Hz, 1H), 7.39 (s, 1H), 7.32−7.28 (m, 5H), 7.25−7.20 (m, 1H), 7.07−6.74 (br, 2H), 6.19 (q, J = 5.3 Hz, 1H), 6.09−6.05 (m, 1H), 4.93−4.87 (m, 1H), 4.20−4.15 (m, 1H), 3.20−2.90 (m, 4H), 2.70 (d, J = 13.3 Hz, 1H), 2.40 (d, J = 13.4 Hz, 1H), 2.24 (s, 1H), 2.01 (d, J = 11.0 Hz, 1H), 1.63−1.57 (m, 3H), 1.49−1.39 (m, 7H), 1.33 (d, J = 7.0 Hz, 5H), 1.25 (s, 20H), 0.87 (td, J = 6.9, 1.4 Hz, 3H). HRMS (ESI) at m/z $[M + H]^+$ Calcd for $C_{35}H_{61}N_7O_3$ is 628.4914. Found: 628.4940.

Biological Evaluation of the Peptides. *Antibacterial Susceptibility Assays.* The MIC and MBC of the peptides **DY-01** to **DY-03** were evaluated against *P. aeruginosa* ATCC-27853 and MRSA ATCC-15187 along with their clinical isolates. MIC was assessed using a modified microtiter plate method based on CLSI guidelines,[37,38] starting at 50 μM and serially diluting to 0.039 μM. Bacterial cultures were prepared at 1.5×10^8 CFU/mL (0.5 McFarland suspension) diluted to 5×10^6 CFU/mL in Luria−Bertani (LB) media. After incubating the microdilution plates at 37 °C for 16 h, colorimetric determination was performed using Alamar blue dye, and optical density was measured at 570 nm with a microplate reader. The Gompertz equation was used to obtain concentration-dependent growth inhibition and MIC for the peptides.[39,40] The *P. aeruginosa* MTCC-424 strain was also used to confirm the MIC assay result with the peptides. MBC was determined by plating 5 μL of bacterial cultures from the MIC plates onto LB agar and incubating at 37 °C; the lowest concentration with no observed colonies was recorded as the MBC.[37] The experiments were conducted in three biological replicates.

Time-Kill Kinetics. The time kill was performed using a standard procedure, as mentioned earlier.[37] Briefly, the cultures of two bacterial species (at OD_{600nm} = 1) were incubated at 37 °C with different concentrations of the peptides and antibiotic control (vancomycin and rifampicin). One hundred and fifty microliters of the cultures were harvested each hour (0−8 h), and absorbance was checked using a spectrophotometer. The OD_{600}nm values were plotted against respective time points. The experiment was conducted in biological triplicates.

Biofilm Disruption and Inhibition Assay. The biofilm quantification assay was performed according to the standard protocol with minor modifications.[37,41] For biofilm disruption and inhibition, the two bacterial species *P. aeruginosa* and MRSA were diluted (1:100, 0.5 McFarland) in tryptic soy broth and 1% glucose (carbohydrate source which acts as a buffer), incubated at 37 °C in a 5% CO_2 incubator. For biofilm disruption, the treatment was given at MIC, 2 × MIC, and 4 × MIC concentrations of the peptides after the first few hours and then incubated for 48 h. For biofilm disruption, the treatment was given at MIC, 2 × MIC, and 4 × MIC concentrations of the peptides after the biofilm formation and further incubated for 24 h to allow the disruption. Later, biofilm quantification was held, and absorbance was measured at 570 nm by a microplate reader. The experiment was performed in three biological replicates.

Checkerboard Assay. *P. aeruginosa* and MRSA were used to evaluate the synergistic efficacy of the peptides in combination with the standard antibiotic rifampicin and vancomycin.[37] The peptide and antibiotic were serially diluted in the microtiter plate vertically and horizontally to create different combinations. Later, 100 μL of culture for the two bacterial species specified above was added in their respective microtiter plates and incubated at 37 °C for 24 h, and absorbance was measured at 570 nm. The wells with ≥80% growth inhibition are considered as MIC values for peptides, antibiotics, and combinations of both. Later, the fractional inhibitory concentration was calculated according to Odds 2003.[42] FICI score is interpreted as ≤0.5, synergy; between 0.5 and 4, no interaction; and ≥4.0, antagonism.

SEM Analysis. The changes in the surface and cell morphologies of *P. aeruginosa* and MRSA were observed via SEM. The analysis was performed as a previously described method with minor modifications.[40,43] The bacterial cultures were harvested at the logarithmic phase (0.5 McFarland), diluted up to 80-fold in LB media, treated with the peptides, and incubated at 37 °C for 6 h. The treated and untreated cultures were then centrifuged at 7000 rpm for 8 min and washed with PBS. Subsequently, the cultures were placed on their respective slides and fixed using a solution of 4% formaldehyde and 2% glutaraldehyde and allowed to incubate overnight at room temperature. After incubation, each slide was washed twice with ethanol (20%, 50%, 70%, and 100%) for 20 min each and then processed for analysis under the microscope according to the established procedure.

Swarming Motility Assay. *P. aeruginosa* shows swarming with different patterns of whirls and jets, which specify the motion in a semisolid medium.[37] Briefly, 3 mL of 0.5% agar was poured into 6-well plates, a sub-MIC value of peptides was added, and later, 2−5 μL of bacterial culture specified above in their stationary phase was dropped at the middle of each well and incubated at 37 °C overnight. The pattern of motion was visualized and analyzed with respect to the untreated sample and antibiotic control (rifampicin). The experiment was performed in three biological replicates.

Hemolysis Assay. The effect of the peptides on red blood cells (rabbit) was determined via a hemolytic assay with some minor modifications.[40] Briefly, 1 mL of whole blood (rabbit) was centrifuged at 10,000 rpm for 5 min; then the pellet was washed five times with PBS and then resuspended in 20 mL of PBS. Further, 100 μL of suspension of red blood cells was aliquoted and incubated with the peptides (20 μM, 10 μM, and 5 μM) for 4 h. Later, samples were centrifuged at 10,000 rpm for 5 min, 100 μL of the sample supernatant was added to their respective microtiter plates of particular concentration, and absorbance was measured using a microtiter plate reader at 577 nm. The experiment was performed in three biological replicates.

MTT Cytotoxicity Assay. The MTT cytotoxicity assay is a colorimetric test used to evaluate the cellular toxicity of peptides on two different cell lines, RAW 264.7 and J774A.1.[37] Both the cell lines were seeded on respective 96-well microtiter plates with 20×10^3 cells per well; Dulbecco's modified Eagle medium supplemented with 10% fetal bovine serum was used as a growth medium for the cell lines and incubated in a CO_2 incubator for 24 h. Further, both cell lines were treated with peptides and rifampicin and incubated in a CO_2 incubator for 16 h. Following this, both the cell lines were treated with MTT solution (2.5 mg/mL) and incubated for 4 h. Later, the solution along with the growth medium was aspirated out of the wells and 100 μL of DMSO was added in each well of the microtiter plate to solubilize the formazan crystals. To calculate the number of viable cells, the absorbance of the microtiter plate was measured at 570 nm using a microtiter plate reader. The experiment was conducted in three biological replicates.

Ex Vivo Infection Model. The ex vivo infection experiment was performed according to a standard procedure.[44] To

https://doi.org/10.1021/acsomega.4c08680
ACS Omega 2025, 10, 2102−2115

evaluate the effect of peptides on an A549 cell infection model with *P. aeruginosa* and MRSA, cells were seeded in 24-well plates at 1.5×10^5 cells/well. After reaching confluence, cells were infected with bacterial suspensions at OD_{600} nm = 0.01 (1.5×10^7 cells/mL, 100-fold infection) and incubated for 1 h. Gentamycin (100 μg/mL) was added and incubated for another hour. The medium was then discarded, and cells were washed twice with 1× PBS. Cells were treated with peptides (**DY-01** to **DY-03**) at 1×-MIC, 2×-MIC, and 4×-MIC, along with standard control vancomycin and rifampicin controls, and incubated in a CO_2 incubator for 16 h. The next day, the medium was discarded, and 500 μL of lysis buffer (0.025% Triton-X 100 + BSA) was added and thoroughly pipetted to ensure complete cell lysis. Serial dilutions of the lysate were prepared in a 1:10 ratio with 1× PBS, plated on agar, and incubated at 37 °C. Bacterial colonies were counted the following day. The experiment was conducted in three biological replicates.

■ ASSOCIATED CONTENT

Supporting Information

The Supporting Information is available free of charge at https://pubs.acs.org/doi/10.1021/acsomega.4c08680.

HPLC chromatograms, NMR and HRMS spectra of **DY01** to **DY-03**, and Table S1 for the checkerboard assay (PDF)

■ AUTHOR INFORMATION

Corresponding Authors

Rajkishor Rai − *Natural Products and Medicinal Chemistry Division, CSIR-Indian Institute of Integrative Medicine, Jammu, Jammu and Kashmir 180001, India; Academy of Scientific & Innovative Research (AcSIR), Ghaziabad 201002, India;* orcid.org/0000-0003-0735-2618; Phone: + 91 0191 2585006; Email: raj@iiim.res; Fax: +91 0191 2586333

Avisek Mahapa − *Infectious Diseases Division, CSIR-Indian Institute of Integrative Medicine, Jammu, Jammu and Kashmir 180001, India; Academy of Scientific & Innovative Research (AcSIR), Ghaziabad 201002, India;* orcid.org/0000-0002-5140-5986; Phone: + 91 0191 2585006; Email: avisek.mahapa@iiim.res.in; Fax: +91 0191 2586333

Authors

Shifa Firdous − *Infectious Diseases Division, CSIR-Indian Institute of Integrative Medicine, Jammu, Jammu and Kashmir 180001, India; Academy of Scientific & Innovative Research (AcSIR), Ghaziabad 201002, India*

Aminur Rahman Sarkar − *Natural Products and Medicinal Chemistry Division, CSIR-Indian Institute of Integrative Medicine, Jammu, Jammu and Kashmir 180001, India; Academy of Scientific & Innovative Research (AcSIR), Ghaziabad 201002, India*

Rakshit Manhas − *Infectious Diseases Division, CSIR-Indian Institute of Integrative Medicine, Jammu, Jammu and Kashmir 180001, India*

Rubina Chowdhary − *Natural Products and Medicinal Chemistry Division, CSIR-Indian Institute of Integrative Medicine, Jammu, Jammu and Kashmir 180001, India; Academy of Scientific & Innovative Research (AcSIR), Ghaziabad 201002, India*

Arti Rathore − *Infectious Diseases Division, CSIR-Indian Institute of Integrative Medicine, Jammu, Jammu and Kashmir 180001, India; Academy of Scientific & Innovative Research (AcSIR), Ghaziabad 201002, India*

Jyoti Kumari − *Infectious Diseases Division, CSIR-Indian Institute of Integrative Medicine, Jammu, Jammu and Kashmir 180001, India; Academy of Scientific & Innovative Research (AcSIR), Ghaziabad 201002, India*

Complete contact information is available at: https://pubs.acs.org/10.1021/acsomega.4c08680

Author Contributions

‖S.F. and A.R.S. contributed equally.

Notes

The authors declare no competing financial interest.

■ ACKNOWLEDGMENTS

This work was supported by an internal institutional grant MLP-110011, extramural grants by the Indian Council of Medical Research, India (ICMR) Research Grant IIRP-2023-0715 (GAP-3160) and Science and Engineering Research Board, India Start-up Research Grant (SERB SRG/2023/000145). S.F., A.R.S., A.R., R.C., and J.K. thank the Council of Scientific and Industrial Research (CSIR), India, and the University Grant Commission (UGC), India, for providing the fellowship grants. R.M. thanks the ICMR for providing the project fellowship. The authors acknowledge ICMR—National Institute for Research in Bacterial Infections (NIRBI), Kolkata, West Bengal, India, for the MDR clinical isolates of *P. aeruginosa* and MRSA. This manuscript has assigned institutional number: CSIR-IIIM/IPR/00773.

■ REFERENCES

(1) Alekshun, M. N.; Levy, S. B. Molecular mechanisms of antibacterial multidrug resistance. *Cell* **2007**, *128* (6), 1037−1050.

(2) Shi, J.; Chen, C.; Wang, D.; Wang, Z.; Liu, Y. The antimicrobial peptide LI14 combats multidrug-resistant bacterial infections. *Commun. Biol.* **2022**, *5* (1), 926.

(3) Zhang, Q.-Y.; Yan, Z.-B.; Meng, Y.-M.; Hong, X.-Y.; Shao, G.; Ma, J.-J.; Cheng, X.-R.; Liu, J.; Kang, J.; Fu, C.-Y. Antimicrobial peptides: mechanism of action, activity and clinical potential. *Mil. Med. Res.* **2021**, *8* (1), 48.

(4) Fjell, C. D.; Hiss, J. A.; Hancock, R. E.; Schneider, G. Designing antimicrobial peptides: form follows function. *Nat. Rev. Drug Discovery* **2012**, *11* (1), 37−51.

(5) Mwangi, J.; Yin, Y.; Wang, G.; Yang, M.; Li, Y.; Zhang, Z.; Lai, R. The antimicrobial peptide ZY4 combats multidrug-resistant Pseudomonas aeruginosa and Acinetobacter baumannii infection. *Proc. Natl. Acad. Sci. U.S.A.* **2019**, *116* (52), 26516−26522.

(6) Li, W.; Separovic, F.; O'Brien-Simpson, N. M.; Wade, J. D. Chemically modified and conjugated antimicrobial peptides against superbugs. *Chem. Soc. Rev.* **2021**, *50* (8), 4932−4973.

(7) de Breij, A.; Riool, M.; Cordfunke, R. A.; Malanovic, N.; de Boer, L.; Koning, R. I.; Ravensbergen, E.; Franken, M.; van der Heijde, T.; Boekema, B. K.; Kwakman, P. H. S.; Kamp, N.; El Ghalbzouri, A.; Lohner, K.; Zaat, S. A. J.; Drijfhout, J. W.; Nibbering, P. H. The antimicrobial peptide SAAP-148 combats drug-resistant bacteria and biofilms. *Sci. Transl. Med.* **2018**, *10* (423), No. eaan4044.

(8) Fremaux, J.; Venin, C.; Mauran, L.; Zimmer, R. H.; Guichard, G.; Goudreau, S. R. Peptide-oligourea hybrids analogue of GLP-1 with improved action in vivo. *Nat. Commun.* **2019**, *10* (1), 924.

(9) Hicks, R. P.; Bhonsle, J. B.; Venugopal, D.; Koser, B. W.; Magill, A. J. De novo design of selective antibiotic peptides by incorporation of unnatural amino acids. *J. Med. Chem.* **2007**, *50* (13), 3026−3036.

(10) Kumari, S.; Carmona, A. V.; Tiwari, A. K.; Trippier, P. C. Amide Bond Bioisosteres: Strategies, Synthesis, and Successes. *J. Med. Chem.* **2020**, *63* (21), 12290−12358.
(11) Grimsey, E.; Collis, D. W. P.; Mikut, R.; Hilpert, K. The effect of lipidation and glycosylation on short cationic antimicrobial peptides. *Biochim. Biophys. Acta, Biomembr.* **2020**, *1862* (8), 183195.
(12) Lin, B.; Hung, A.; Singleton, W.; Darmawan, K. K.; Moses, R.; Yao, B.; Wu, H.; Barlow, A.; Sani, M.-A.; Sloan, A. J.; Hossain, M. A.; Wade, J. D.; Hong, Y.; O'Brien-Simpson, N. M.; Li, W. The effect of tailing lipidation on the bioactivity of antimicrobial peptides and their aggregation tendency: Special Issue: Emerging Investigators. *Aggregate* **2023**, *4*, No. e329.
(13) Armas, F.; Di Stasi, A.; Mardirossian, M.; Romani, A. A.; Benincasa, M.; Scocchi, M. Effects of Lipidation on a Proline-Rich Antibacterial Peptide. *Int. J. Mol. Sci.* **2021**, *22* (15), 7959.
(14) Puszko, A. K.; Sosnowski, P.; Pułka-Ziach, K.; Hermine, O.; Hopfgartner, G.; Lepelletier, Y.; Misicka, A. Urea moiety as amide bond mimetic in peptide-like inhibitors of VEGF-A(165)/NRP-1 complex. *Bioorg. Med. Chem. Lett.* **2019**, *29* (17), 2493−2497.
(15) Ghosh, A. K.; Brindisi, M. Urea Derivatives in Modern Drug Discovery and Medicinal Chemistry. *J. Med. Chem.* **2020**, *63* (6), 2751−2788.
(16) Claudon, P.; Violette, A.; Lamour, K.; Decossas, M.; Fournel, S.; Heurtault, B.; Godet, J.; Mély, Y.; Jamart-Grégoire, B.; Averlant-Petit, M. C.; Briand, J.-P.; Duportail, G.; Monteil, H.; Guichard, G. Consequences of isostructural main-chain modifications for the design of antimicrobial foldamers: helical mimics of host-defense peptides based on a heterogeneous amide/urea backbone. *Angew. Chem., Int. Ed. Engl.* **2010**, *49* (2), 333−336.
(17) Charifson, P. S.; Grillot, A.-L.; Grossman, T. H.; Parsons, J. D.; Badia, M.; Bellon, S.; Deininger, D. D.; Drumm, J. E.; Gross, C. H.; LeTiran, A.; Liao, Y.; Mani, N.; Nicolau, D. P.; Perola, E.; Ronkin, S.; Shannon, D.; Swenson, L. L.; Tang, Q.; Tessier, P. R.; Tian, S.-K.; Trudeau, M.; Wang, T.; Wei, Y.; Zhang, H.; Stamos, D. Novel Dual-Targeting Benzimidazole Urea Inhibitors of DNA Gyrase and Topoisomerase IV Possessing Potent Antibacterial Activity: Intelligent Design and Evolution through the Judicious Use of Structure-Guided Design and Structure−Activity Relationships. *J. Med. Chem.* **2008**, *51* (17), 5243−5263.
(18) Grillot, A.-L.; Tiran, A. L.; Shannon, D.; Krueger, E.; Liao, Y.; O'Dowd, H.; Tang, Q.; Ronkin, S.; Wang, T.; Waal, N.; Li, P.; Lauffer, D.; Sizensky, E.; Tanoury, J.; Perola, E.; Grossman, T. H.; Doyle, T.; Hanzelka, B.; Jones, S.; Dixit, V.; Ewing, N.; Liao, S.; Boucher, B.; Jacobs, M.; Bennani, Y.; Charifson, P. S. Second-generation antibacterial benzimidazole ureas: discovery of a preclinical candidate with reduced metabolic liability. *J. Med. Chem.* **2014**, *57* (21), 8792−8816.
(19) Yule, I. A.; Czaplewski, L. G.; Pommier, S.; Davies, D. T.; Narramore, S. K.; Fishwick, C. W. G. Pyridine-3-carboxamide-6-yl-ureas as novel inhibitors of bacterial DNA gyrase: structure based design, synthesis, SAR and antimicrobial activity. *Eur. J. Med. Chem.* **2014**, *86*, 31−38.
(20) Chowdhary, R.; Mubarak, M. M.; Kantroo, H. A.; Ur Rahim, J.; Malik, A.; Sarkar, A. R.; Bashir, G.; Ahmad, Z.; Rai, R. Synthesis, Characterization, and Antimicrobial Activity of Ultra-Short Cationic β-Peptides. *ACS Infect. Dis.* **2023**, *9* (7), 1437−1448.
(21) Horne, W. S.; Gellman, S. H. Foldamers with heterogeneous backbones. *Acc. Chem. Res.* **2008**, *41* (10), 1399−1408.
(22) Wani, N. A.; Singh, G.; Shankar, S.; Sharma, A.; Katoch, M.; Rai, R. Short hybrid peptides incorporating β- and γ-amino acids as antimicrobial agents. *Peptides* **2017**, *97*, 46−53.
(23) Shankar, S.; Jyothi, D.; Ur Rahim, J.; Pal, P. C.; Singh, U. P.; Rai, R. Conformation of Achiral α/β Hybrid Peptides Containing Glycine and 1-Aminocyclohexaneacetic Acid. *ChemistrySelect* **2022**, *7*, No. e202104453.
(24) Kumar, D.; Rahman Sarkar, A.; Iqbal Andrabi, N.; Assim Haq, S.; Ahmed, M.; Kumar Shukla, S.; Ahmed, Z.; Rai, R. Synthesis, characterization, and anti-inflammatory activity of tetrahydropiperine, piperic acid, and tetrahydropiperic acid via down regulation of NF-κB pathway. *Cytokine* **2024**, *178*, 156578.
(25) Murray, C. J. L.; Ikuta, K. S.; Sharara, F.; Swetschinski, L.; Robles Aguilar, G.; Gray, A.; Han, C.; Bisignano, C.; Rao, P.; Wool, E.; et al. Global burden of bacterial antimicrobial resistance in 2019: a systematic analysis. *Lancet* **2022**, *399* (10325), 629−655.
(26) Chu, H. L.; Yu, H. Y.; Yip, B. S.; Chih, Y. H.; Liang, C. W.; Cheng, H. T.; Cheng, J. W. Boosting salt resistance of short antimicrobial peptides. *Antimicrob. Agents Chemother.* **2013**, *57* (8), 4050−4052.
(27) Mandal, S. M.; Roy, A.; Ghosh, A. K.; Hazra, T. K.; Basak, A.; Franco, O. L. Challenges and future prospects of antibiotic therapy: from peptides to phages utilization. *Front. Pharmacol.* **2014**, *5*, 105.
(28) Hancock, R. E. Cationic peptides: effectors in innate immunity and novel antimicrobials. *Lancet Infect. Dis.* **2001**, *1* (3), 156−164.
(29) Werner, H. M.; Horne, W. S. Folding and function in α/β-peptides: targets and therapeutic applications. *Curr. Opin. Chem. Biol.* **2015**, *28*, 75−82.
(30) Mwangi, J.; Kamau, P. M.; Thuku, R. C.; Lai, R. Design methods for antimicrobial peptides with improved performance. *Zool. Res.* **2023**, *44* (6), 1095−1114.
(31) Mirghani, R.; Saba, T.; Khaliq, H.; Mitchell, J.; Do, L.; Chambi, L.; Diaz, K.; Kennedy, T.; Alkassab, K.; Huynh, T.; Elmi, M.; Martinez, J.; Sawan, S.; Rijal, G. Biofilms: Formation, drug resistance and alternatives to conventional approaches. *AIMS Microbiol.* **2022**, *8* (3), 239−277.
(32) Taheri-Araghi, S. Synergistic action of antimicrobial peptides and antibiotics: current understanding and future directions. *Front. Microbiol.* **2024**, *15*, 1390765.
(33) Mba, I. E.; Nweze, E. I. Antimicrobial Peptides Therapy: An Emerging Alternative for Treating Drug-Resistant Bacteria. *Yale J. Biol. Med.* **2022**, *95* (4), 445−463.
(34) Xuan, J.; Feng, W.; Wang, J.; Wang, R.; Zhang, B.; Bo, L.; Chen, Z.-S.; Yang, H.; Sun, L. Antimicrobial peptides for combating drug-resistant bacterial infections. *Drug Resistance Updates* **2023**, *68*, 100954.
(35) Mohamed, M. F.; Abdelkhalek, A.; Seleem, M. N. Evaluation of short synthetic antimicrobial peptides for treatment of drug-resistant and intracellular Staphylococcus aureus. *Sci. Rep.* **2016**, *6*, 29707.
(36) Nguyen, H. M.; Graber, C. J. Limitations of antibiotic options for invasive infections caused by methicillin-resistant Staphylococcus aureus: is combination therapy the answer? *J. Antimicrob. Chemother.* **2010**, *65* (1), 24−36.
(37) Manhas, R.; Rathore, A.; Havelikar, U.; Mahajan, S.; Gandhi, S. G.; Mahapa, A. Uncovering the potentiality of quinazoline derivatives against Pseudomonas aeruginosa with antimicrobial synergy and SAR analysis. *J. Antibiot.* **2024**, *77* (6), 365−381.
(38) Humphries, R.; Bobenchik, A. M.; Hindler, J. A.; Schuetz, A. N. Overview of Changes to the Clinical and Laboratory Standards Institute Performance Standards for Antimicrobial Susceptibility Testing, M100, 31st Edition. *J. Clin. Microbiol.* **2021**, *59* (12), No. e0021321.
(39) Lambert, R. J.; Pearson, J. Susceptibility testing: accurate and reproducible minimum inhibitory concentration (MIC) and non-inhibitory concentration (NIC) values. *J. Appl. Microbiol.* **2000**, *88* (5), 784−790.
(40) Sarkar, A. R.; Kumari, J.; Rathore, A.; Chowdhary, R.; Manhas, R.; Firdous, S.; Mahapa, A.; Rai, R. Antimicrobial activity of α/β hybrid peptides incorporating tBu-β3,3Ac6c against methicillin-resistant Staphylococcus aureus. *J. Antibiot.* **2024**, *77*, 794−801.
(41) Mahapa, A.; Samanta, G. C.; Maiti, K.; Chatterji, D.; Jayaraman, N. Mannopyranoside glycolipids inhibit mycobacterial and biofilm growth and potentiate isoniazid inhibition activities in M. smegmatis. *ChemBioChem* **2019**, *20* (15), 1966−1976.
(42) Odds, F. C. Synergy, antagonism, and what the chequerboard puts between them. *J. Antimicrob. Chemother.* **2003**, *52*, 1.
(43) Monson, B. K.; Stringham, J.; Jones, B. B.; Abdel-Aziz, S.; Cutler Peck, C. M.; Olson, R. J. Scanning electron microscopy visualization of methicillin-resistant Staphylococcus aureus after

https://doi.org/10.1021/acsomega.4c08680
ACS Omega 2025, 10, 2102−2115

contact with gatifloxacin with and without preservative. *J. Ocul. Pharmacol. Ther.* **2010**, *26* (2), 133−136.
(44) Crabbe, A.; Liu, Y.; Matthijs, N.; Rigole, P.; De La Fuente-Nunez, C.; Davis, R.; Ledesma, M. A.; Sarker, S.; Van Houdt, R.; Hancock, R. E. W.; Coenye, T.; Nickerson, C. A. Antimicrobial efficacy against Pseudomonas aeruginosa biofilm formation in a three-dimensional lung epithelial model and the influence of fetal bovine serum. *Sci. Rep.* **2017**, *7*, 43321.

https://doi.org/10.1021/acsomega.4c08680
ACS Omega 2025, 10, 2102−2115